Proceedings of the 2005 IEEE
International Conference on Robotics and Automation
Barcelona, Spain, April 2005

Mimicry of Sharp Turning Behaviours in a Robotic Fish*

Jindong Liu
Department of Computer Science
University of Essex,
Colchester, Essex, CO4 3SQ, U.K.
jliua@essex.ac.uk

Huosheng Hu
Department of Computer Science
University of Essex,
Colchester, Essex, CO4 3SQ, U.K.
hhu@essex.ac.uk

***Abstract* - In nature, fish has astonishing swimming ability after thousands years of evolution. To realise fish-like swimming behaviours by a robotic system poses tremendous challenges, especially for the C-shape turning (CST). This requires fully understanding of fish biomechanics and the way to mimic it. Based on observations of fish swimming, this paper presents a new kinematics model to mimic the CST behaviour in a robotic fish with a 4-DOF (degrees of freedom) tail. The simulated and the real experiments are conducted to show the theoretic feasibility. Both behaviour analyses and hydrodynamics features between the robotic fish and the real fish are presented to show the performance.**

Index Terms - Robotic fish, C-shape sharp turn, kinematics model.

I. INTRODUCTION

It is well known that the tuna swims with high speed and high efficiency, the pike accelerates in a flash and the eel can swim skilfully into narrow holes. Such astonishing swimming ability inspired the researchers to improve the performance of aquatic man-made robotic systems, namely Robotic Fishes. Instead of the conventional rotary propeller used in ship or underwater vehicles, a robotic fish relies on the undulation movement to provide the main energy. The observation on a real fish shows that this kind of propulsion is less noisy, more effective, and manoeuvrable than the propeller-based propulsion. So, the robotic fish could be used in many marine and military fields such as exploring fish behaviours, detecting the leakage in oil pipelines, sea bed exploration, mine countermeasures, robotics education, etc.

Most of previous robotic fish projects were focused on the hydrodynamics mechanism of fish-like swimming (especially the steady straight swimming[1]), the special skin material [2] and the mechanical structure of robotic fish models[3][4][9]. However, a real fish has many different manoeuvrable swimming modes, and swimming at uniform velocities along a straight path is rather exceptional [5]. In other words, *unsteady behaviours* such as C-sharp turn, S-sharp turn, fast starts, brake and burst are very common. Although many biologists have studied the energy cost, fish muscle feature and the kinematics of the whole fish body [7] from many years, few robotic researchers have built models to activate these behaviours in robots. The main challenges lie in the limitation of mechanics of current robotic fish tails on the undulation movement. There are no exact kinematics and hydrodynamics mechanism for describing these complex swimming modes. So, modelling unsteady fish behaviours in a robotic fish remains a real challenge for us.

The aim of our research project is to design and build an autonomous robotic fish that would have two main features: (i) to swim like a real fish, and (ii) to realise autonomous navigation [8]. At this stage, we decompose the fish-like swimming motion into *basic swimming behaviours* and then build a swimming library for the controller to generate complete swimming trajectories. This paper is focused on how the one of basic fish swimming behaviours, CST, is realised in a robotic fish. Compared with the normal turning which applies an offset on normal flapping of the fish tail, CST is faster and more effective. For example, an adult carp can turn backward in only half second. This fast turning behaviour is very useful for many real-world applications, which motivates us to work on the issue.

The rest of this paper is organized as follows. Section II describes the schematic structure of the robotic fish and the basic idea on how to model fish behaviours by a 4-DOF tail. Section III presents a kinematics model for the CST behaviour, which is based on the observation and the mechanical structure of our robotic fishes. Section IV addresses the hydrodynamics analysis on the kinematics equations proposed. In Section V, some simulated and real experiments are given to show the feasibility and performance of the proposed CST model, including relative comparison between the simulated and the real fish. Finally, conclusions and future work are described in Section VI.

II. SCHEMATIC STRUCTURE OF THE ROBOTIC FISH

A. Schematic structure

We have built several robotic fishes for our research at Essex. Fig. 1 shows the one used for the experiment here and its schematic structure. It is about 800mm long and has 6 powerful R/C servo motors. Four motors are concatenated together in the tail to act as 4 joints and other 2 servo motors are fixed in the head to drive two pectoral fins to slap up and down. The control box contains a computer board which is responsible for sampling data from sensors, transferring diagnostic information via a RF link, processing data, making decisions and sending out signals to control servo motors. The tail part (after pectoral fins) is waterproof by using a kind of foldable plastic with metal ribs.

On the back of the fish body, a dorsal fin is fixed vertically to keep the fish from swaging. The high quality of servo motors and the very soft structure of the tail make it possible for the robotic fish to bend its body at a big angle in a short time (about 90°/0.20sec). Note that the implementation of such an unsteady motion is novel and has not been implemented so far.

* This work is supported by London Aquarium Ltd.

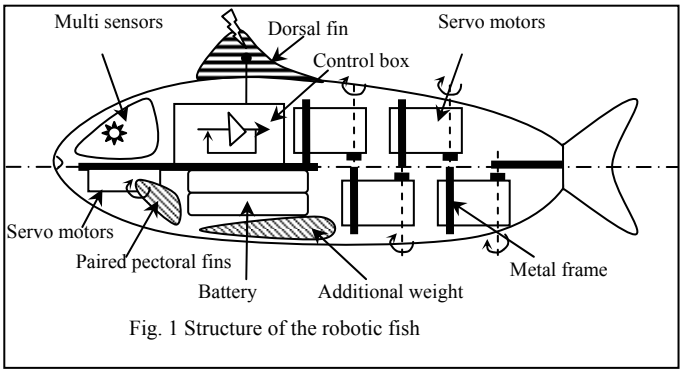

Fig. 1 Structure of the robotic fish

B. Realise fish behaviours by 4 joints

It is clear that the variety of fish behaviours are mainly achieved by changing the body shape continuously, i.e. the undulation feature of its tail. To realise these in a 4-joint robotic fish, we decompose each behaviour into a sequence of *tail gestures* in a sequence of time frames, as shown in Fig. 2. Assume that the robotic fish realises one behaviour if its tail can approximate the tail gesture of that behaviour in each moment of the sequence under a permitted error.

Fig. 3 shows an approximation method which uses four rigid joints to approximate an ideal wave, i.e. a tail gesture. So, the problem of how to realise fish behaviours in a robotic fish becomes how to generate the *joint-end-point trajectory* of the four joints to approximate the gesture sequence of the fish behaviour.

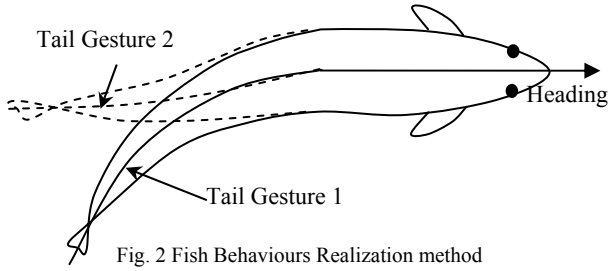

Fig. 2 Fish Behaviours Realization method

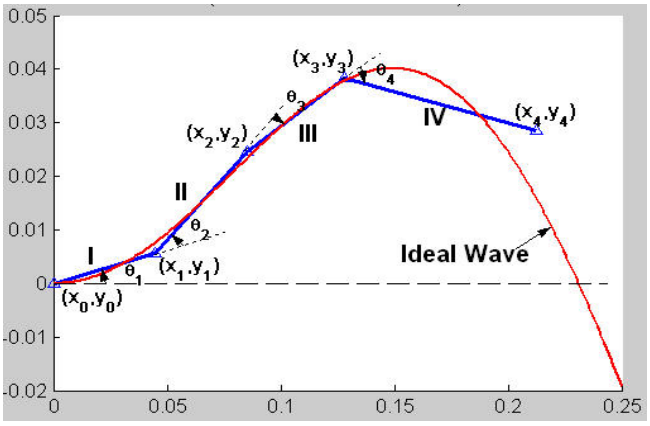

Fig. 3 An example of tail gesture approximation

III KINEMATICS MODEL ON THE FISH-LIKE C-SHAPE SHARP TURNING

Although many biologists have investigated the fish sharp turn, they mainly focused on the wake dynamics [10] and the kinematics of whole fish body in the earth coordination. Even now there is no equation to describe such a sharp turn due to its complexity. To realise the sharp turn movement in the robotic fish, we proposed a novel method to generate the approximate joint-end-point trajectory in the coordinates in which the fish tail moves relative to the fish head, i.e. relative coordinates.

Fig. 4 is a CST sequence recorded from an adult carp [1]. We divide it into two stages: *shrink stage* and *release stage*. In the shrink stage (about from 0 ms to 30 ms in Fig. 4), the tail bends toward one side very quickly. The quicker the sharp turn, the bigger the tail bending angle is. In the release stage, the tail unbends in a relatively slow speed from the middle section of the body to the tail tip.

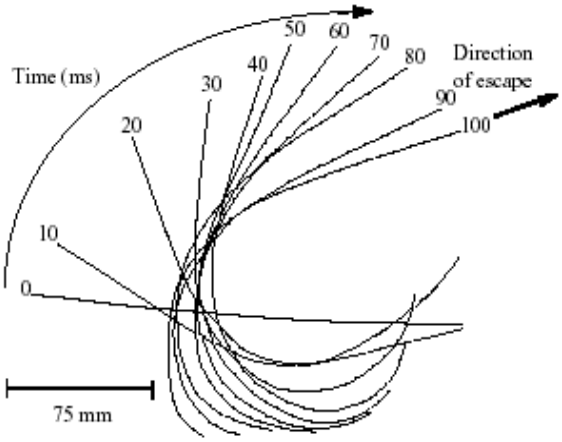

Fig. 4 A C-shape fast turn sequence **[3]**

The gesture sequence of a sharp turn looks as if that the fish embraces a circle whose centre and radius changes depending on time. Based on this observation, we propose a kinematics model on the joint-end-point trajectory as shown in (1), i.e. a circle function.

$$[x - x_c(t)]^2 + [y - y_c(t)]^2 = y_c^2(t) \qquad (1)$$

where $x_c(t)$ and $y_c(t)$ form the trajectory of the circle centre in terms of time.

The centre of the circle changes respect to time and it is tangent to x-axis. So, $y_c(t)$ is equal to the radius of the circle. We suppose this trajectory could be divided into two secondary curves (Fig. 5) - curve (AB) and curve (BC). The point A represents the centre of the initial circle when the tail just starts to shrink, the point B is the centre of the transfer circle when the tail finishes the shrink stage and enters the release stage and the point C is the centre of the end circle which is at the end of the release stage.

The first derivative to y of two curves in point B equal to 0. So, the equation of (AB) and (BC) can be determined if given the coordinates of points A, B, C. So, the relationship between $x_c(t)$ and $y_c(t)$ is described in Eqn. (2).

$$x_c(t) = \begin{cases} a_{11} y_c^2(t) + a_{12} y_c(t) + a_{13} & t \in [t_0, t_1) \\ a_{21} y_c^2(t) + a_{22} y_c(t) + a_{23} & t \in [t_1, t_2] \end{cases} \qquad (2)$$

where

$$[a_{11} \quad a_{12} \quad a_{13}] = [cx_0 \quad cx_1 \quad 0] * \begin{bmatrix} cy_0^2 & cy_1^2 & 2cy_1 \\ cy_0 & cy_1 & 1 \\ 1 & 1 & 0 \end{bmatrix}^{-1}$$

and

$$[a_{21} \quad a_{22} \quad a_{23}] = [cx_1 \quad cx_2 \quad 0] * \begin{bmatrix} cy_1^2 & cy_2^2 & 2cy_1 \\ cy_1 & cy_2 & 1 \\ 1 & 1 & 0 \end{bmatrix}^{-1}$$

$y_c(t)$ is the mapping between y_c and time t, i.e.:

$$y_c(t) = \begin{cases} cy_1 + (t-t_1)^k (cy_0 - cy_1)/(t_0 - t_1)^k & t \in [t_0, t_1) \\ cy_1 + (t-t_1)^m (cy_1 - cy_2)/(t_2 - t_1)^m & t \in [t_1, t_2] \end{cases}$$

where $cx_i, cy_i, t_i, (i = 0,1,2), k, m$ are parameters to decide the feature of the sharp turn such as the tail shape, the bending speed and the maximum bending angle, etc.

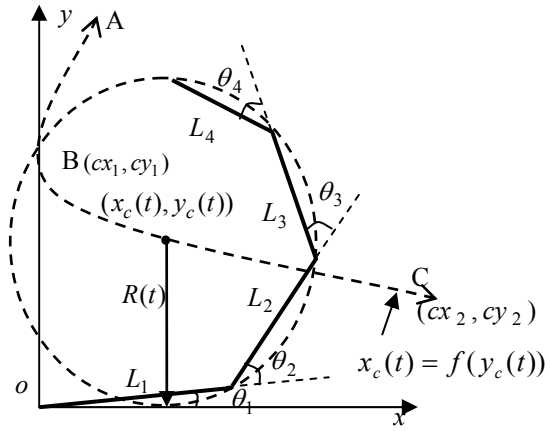

Fig. 5 The joint-end trajectory of C-shape fast turn

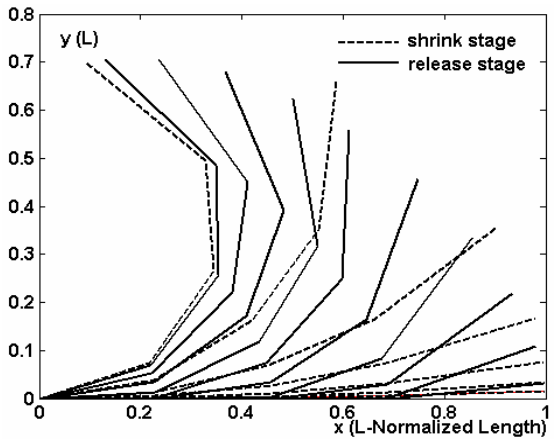

Fig. 6 The tail bending sequence in a fast turn

Fig. 5 shows the computation of joint angles $\theta_i (i = 1...4)$ and we skip it here due to easy deduction. The curve (ABC) is the trajectory of the centre of the circle and the curve (AB) is the shrink stage ($t \in [t_0, t_1)$) while the curve (BC) is the release stage ($t \in [t_1, t_2]$). Fig. 6 is the tail bending sequence of a sharp turn in which the original point is the conjunction of the head and the tail. Note that the tail length is normalized to 1. Fig. 7 is the joint angle curve of the same fast turn. It is clear that there is a sharp increase in the shrink stage (t<30) and a slower decrease in the release stage (30<t<100).

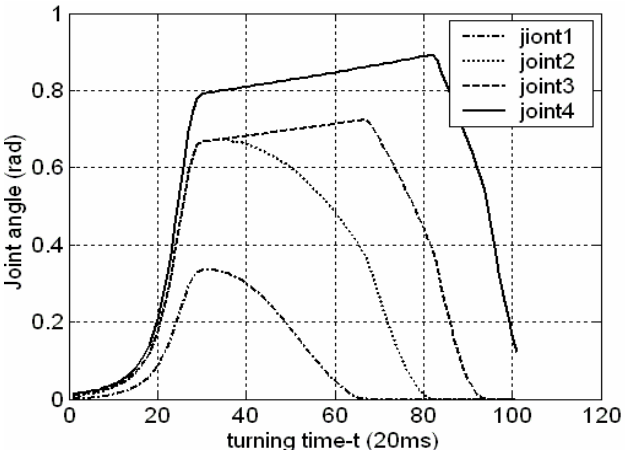

Fig. 7 The joint angle curves in a fast turn

IV. HYDRODYNAMIC ANALYSIS

To prove the feasibility of the kinematics model for the CST behaviour, we analysis the hydrodynamics feature of the proposed kinematics model based on the mechanical feature of the robotic fish. Here, we define two coordinate systems: *fish body coordinate system* (FBCS from now on) (Fig. 8) and *head-fixed relative coordinate system* (HFRCS from now on), as shown in Fig. 9. The former is a one-dimension coordinate system and the midline of fish back builds up on it. The head tip is defined as the original point and the total fish length is normalized to 1. In Fig. 8, the point "a" is the connection between the rigid fish head and the flexible fish tail. The point "b" is the connection between the tail and the soft fan.

In the HFRCS, we suppose that the fish head (from 0 to a in FBCS) is fixed in the x-axis and the fish tail (from a to b in FBCS) moves relative to its head. In Fig. 9, the solid bold line represents the fish body which fits to the circle outline. The circle function is defined by (3), which is the parameter of Equation (1).

$$\begin{cases} x(t,\theta) = R_c(t)\cos\theta + x_c(t) \\ y(t,\theta) = R_c(t)\sin\theta + y_c(t) \end{cases} \quad \theta \in [-\pi/2, -\pi/2 + \theta_c(t)] \quad (3)$$

Because $\theta_c(t)R_c(t) + x_c(t) = b - a$ and $R_c(t) = y_c(t)$, then we get:

$$\begin{cases} x(t,\theta) = y_c(t)\cos\theta + x_c(t) \\ y(t,\theta) = y_c(t)\sin\theta + y_c(t) \end{cases} \quad \theta \in \left[\frac{-\pi}{2}, \frac{-\pi}{2} + \frac{(b-a-x_c(t))}{y_c(t)}\right] \quad (4)$$

The coordination of the mass centre $(x_w(t), y_w(t))$ could be deduced as follows

$$x_w(t) = \frac{1}{M}\left[\int_0^a x\rho(l)dl + \int_a^{a+x_c(t)} x\rho(l)dl + \int_{a+x_c(t)}^b x\rho(l)dl\right] \quad (5)$$

where M is the mass of the fish, l is the normalized fish length and $\rho(l)$ is the density function depend on the fish length l.

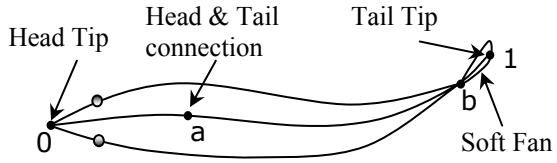

Fig. 8 Fish body coordinate system (FBCS)

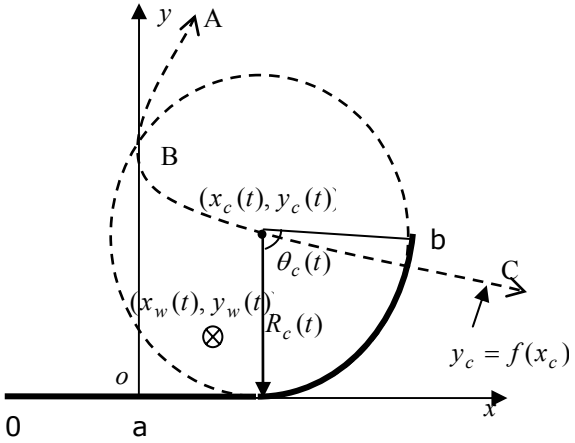

Fig. 9 Head-fixed relative coordinate system (HFRCS)

When $l \in [0, a+x_c(t)]$ then $l = x + a$ and when $l \in [a+x_c(t), b]$ then $l = x_c(t) + R_c(t)\theta$, $dl = R_c(t)d\theta$, so (5) could be rewritten as:

$$x_w(t) = \frac{1}{M}\left[\begin{array}{l}\int_{-a}^{x_c(t)} x\rho(x+a)dx + \\ \int_{-\pi/2}^{-\pi/2+\theta_c(t)} \left[y_c(t)\cos\theta + x_c(t)\right]\rho(x_c(t)+R_c(t)\theta)R_c(t)d\theta\end{array}\right]$$

Similarly:

$$y_w(t) = \frac{1}{M}\left[\begin{array}{l}\int_{-a}^{x_c(t)} y\rho(x+a)dx + \\ \int_{-\pi/2}^{-\pi/2+\theta_c(t)} \left[y_c(t)\cos\theta + y_c(t)\right]\rho(x_c(t)+R_c(t)\theta)R_c(t)d\theta\end{array}\right]$$

This is because $y = 0$ when $x \in [-a, x_c(t)]$, so we have:

$$y_w(t) = \frac{1}{M}\int_{-\pi/2}^{-\pi/2+\theta_c(t)} \left[y_c(t)\cos\theta + y_c(t)\right]\rho(x_c(t)+R_c(t)\theta)R_c(t)d\theta$$

Suppose the main energy for the fish sharp turn comes from the reactive force $F(l,t)$ from the water and ignore the interaction force between fish muscles. This supposition is feasible in the robotic fish because the connections between tail joints are rigid beams with ignorable elastic coefficient. The direction of $F(l,t)$ is vertical to the fish body and its magnitude is proportional to added-mass $m_a(l)$ and tail acceleration $a(l,t)$. Neglect the reactive forces of water in the tangential direction. To simplify the problem, we consider the water resistance $D(l,t)$ only which is caused by turning movement and neglect the linear movement's resistance. All force acting on the fish in CST turning is shown in Fig. 10.

The added-mass of a cross-section could be calculated as [6]:

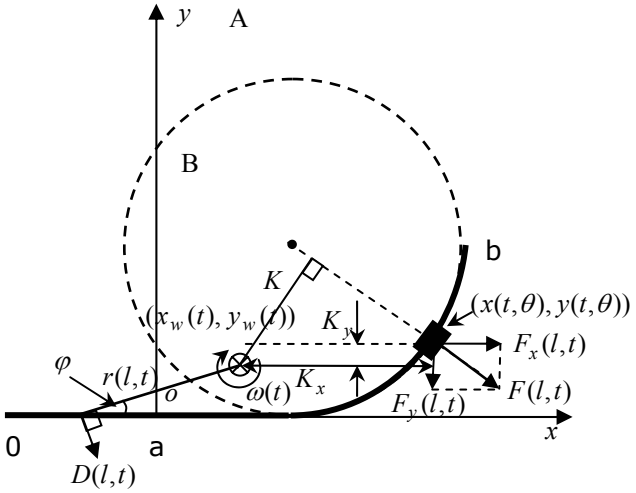

Fig. 10 Moment analysis of the robotic fish

$$m_a(l) = 0.25\pi\rho_w h^2 \tag{8}$$

where ρ_w is the water density and h is the cross-section depth, i.e. the fish height in total length L.

Suppose $a(l,t) \cong R_c''(t) = y_c''(t)$, $F(l,t)$ could be expressed as: $F(l,t) = \eta m_a(l) y_c''(t)$, where η is a constant coefficient.

Considering a thin slab of the fish tail (the black rectangle in Fig. 10), its coordination is $(x(t,\theta), y(t,\theta))$ in the HFRCS and the moment of $F(l,t)$ to the mass centre is:

$$T_F(l,t) = F(l,t)K \tag{9}$$

where K is the arm distance.

We decompose $F(l,t)$ into $F_x(l,t)$ and $F_y(l,t)$ in x-direction and y-direction, (9) could be written as:

$$\begin{aligned} T_F(l,t) &= F_x(l,t)K_y + F_y(l,t)K_x \\ &= F(l,t)\sin\theta\left[x(t,\theta) - x_w(t)\right] + F(l,t)\cos\theta\left[y(t,\theta) - y_w(t)\right] \end{aligned} \tag{10}$$

Similarly, the water resistance $D(l,t)$ could be calculated as:

$$D(l,t) = 0.5\rho_w C_d\left[\omega(t)r(l,t)\right]^2 A(l,t)$$

where $\omega(t)$ is the angular velocity of the robotic fish and $A(l,t) = 0.5\pi h\cos\varphi dl$ is the effective resistance area.
The moment of $D(l,t)$ to the mass centre is written as:

$$T_D(l,t) = D(l,t)r(l,t)$$

The total moment is calculated as:

$$T(t) = \int_0^b T_F(l,t)dl - \int_0^b T_D(l,t)dl$$

The moment of inertia of the fish body to its mass centre could be calculated as follows:

$$I(t) = \int_{-a}^{x_c(t)} \rho(x+a)Rw_1 dx + \int_{-\pi/2}^{-\pi/2+\theta_c(t)} \rho(\theta)Rw_2 R_c(t)d\theta$$

where $\begin{cases} Rw_1 = y_w^2(t) + (x - x_w(t))^2 \\ Rw_2 = (x(t,\theta) - x_w(t))^2 + (y(t,\theta) - y_w(t))^2 \end{cases}$

and $\rho(\theta) = x_c(t) + R_c(t)\theta$.

Now, the angular acceleration of the fish body relative to the mass centre could be obtained from:

$$a_w(t) = T(t)/I(t) \qquad (12)$$

The angular velocity $\omega(t)$ and the turning angle could be calculated by the integration of $a_w(t)$.

V. Experimental Results

A. Simulation results

To compare the kinematics feature of the proposed CST model with the real fish sharp turning, we calculated the angular acceleration, velocity and turning angle by Matlab. For computation convenience, the fish mass, fish dimension, acceleration, velocity and time are normalized. Suppose that a robotic fish has uniform density in its body direction, and swims in quasi-static water. The effect of its dorsal fins and pectoral fins can be ignored. The following kinematics parameters are selected in our experiments:

$$cx_0 = 0.14, cx_1 = 0, cx_2 = 0.595$$
$$cy_0 = 20, cy_1 = 0.245, cx_2 = 0.35$$
$$t_0 = 0, t_1 = 0.3, t_2 = 1$$
$$a = 0.3, b = 0.95, k = 3, m = 0.5$$

The corresponding simulated result is shown in Fig. 11. It should be noticed that the units of axes have no real physical meanings. Compared with one recorded result of a carp fish (Fig. 12), it is clear that they are very similar. Due to the multiplicity of fish and the lack of recorded real fish turning, it is impossible and also pointless to make quantitative comparison between the real fish and the simulated ones. We only make some qualitative analysis here. The transfer moment from a shrink stage to a release stage in Fig. 12 is 30. So we set the same value in the simulation ($t_1 = 0.3$) for more accurate comparison.

It is easy to see that the peak of the angular velocity occurred in about the middle way before the transfer moment in both figures. The velocity decreases to the half of the peak in the transfer moment and continues to drop until zero in the release stage. The increase of turning angle is faster in the shrink stage than in the release stage. Although the shrink stage is much shorter than the release stage, the fish has finished over half of total turning angle at the end of the shrink stage. So, the proposed kinematics for the robotic fish is reasonable according to the simulation result.

To achieve different turning angles and difference turning velocities, we could adjust the parameters in the kinematics model. Fig. 13 shows an example; it illustrates the relationship between parameter cy_0 and the turning angle with the same configuration of other parameters as above.

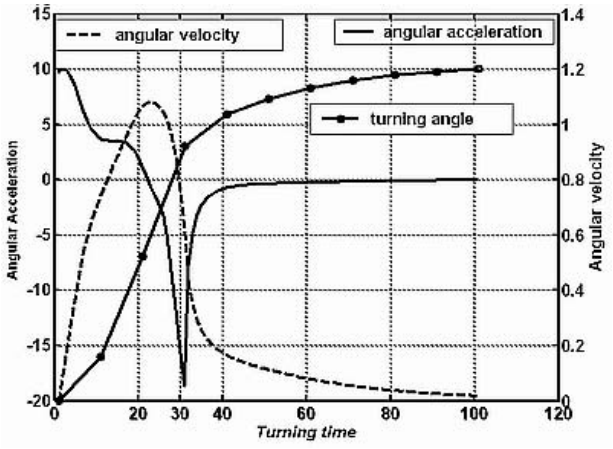

Fig. 11 Simulated angular acceleration, velocity and turning angle of C-shape sharp turn

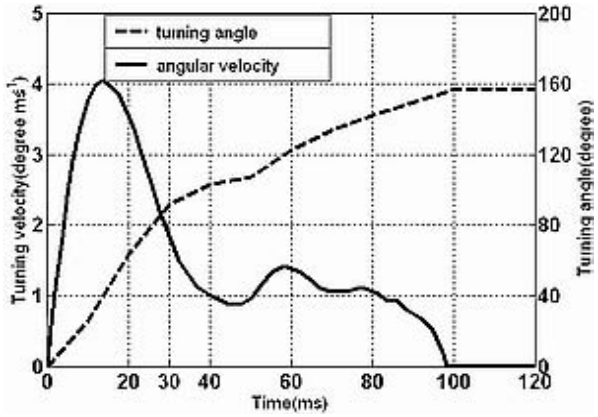

Fig. 12 The angular velocity and turning angle of a carp's C-shape sharp turn (recorded from [3])

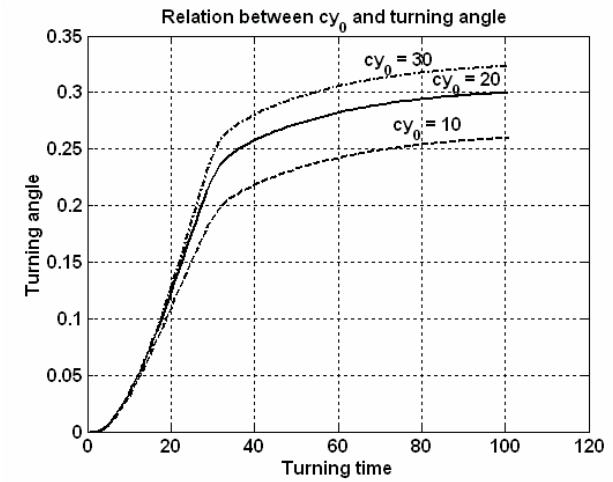

Fig. 13 The relation between cy_0 and turning angle

B. Robotic fish test results

To further prove the accuracy of the kinematics model, we applied it to our robotic fish and tested it in water. Its performance is very similar to a real fish and could achieve the maximum turning velocity of 110 degrees per second. The average turning angle curve is shown in Fig. 14.

Since the parameter configuration is set to be slow sharp turn, this limits the total turning time in about 2 second because of the mechanical limitation of the tail. The shrink stage is finished just before 1s. There is recoil after the maximum turning angle. The final turning angle is about 65 degrees. Fig. 15 is a snapshot of CST of the robotic fish.

The shape of the curve is similar to the simulated result except for the recoil which is caused by uneven mass distribution in the robotic fish body. However, in the global view, the turning velocity of the robotic fish is already very high, compared with the normal turning (max 20 degrees per second). This could be even higher when better mechanical design and fast sharp turn configuration are in position.

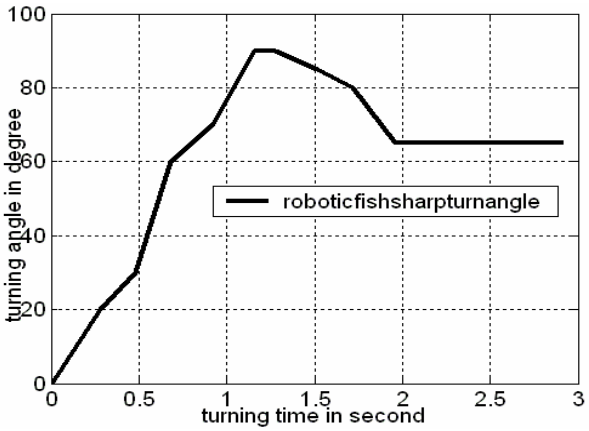

Fig. 14 The average turning angle of CST of a robotic fish

Fig. 15 A snapshot of CST of our robotic fish

VI. Conclusions and Future Work

The experimental results from both the simulated and the real robotic fish made it clear that our kinematics model built for the fish-like CST behaviour is reasonable and can be easily realised in a 4-DOF robotic fish. Although the robotic fish can not realise the fast turning velocity as a real fish due to its engineering limitation, it can achieve a large turning angle in a shorter time than the normal turning.

The research conducted is encouraging and more research on the fish behaviour is needed in order to improve the capability of the robotic fish. In the next stage, we plan to optimise the parameters of a sharp CST turning and at the same time realise the sharp S-shape turn (SST) behaviour as well.

Acknowledgments

Our thanks go to Ian Dukes, Rob Knight and George Francis at Essex for their contribution toward the project.

References

[1] K. Streitlien, G. S. Triantafyllou, and M. S. Triantafyllou, "Efficient foil propulsion through vortex control," AIAA Journal, Vol. 34, 1996, pages 2315–2319.

[2] S. Guo, T. Fukuda, Norihiko KATO, Keisuke OGURO. "Development of Underwater Microrobot Using ICPF Actuator". Proceedings of the IEEE International Conference on Robotics and Automation, May 1998, pages 1829-1834.

[3] http://www.mhi.co.jp/enews/e_0898.html

[4] http://www.nmri.go.jp/eng/khirata/fish

[5] J.J. Videler, "Fish Swimming", London, UK: Chapman & Hall.1993. pages 121.

[6] J.J. Videler, "Fish Swimming", London, UK: Chapman & Hall.1993. pages 19.

[7] Igor L. Y. Spierts, Johan L. Van Leeuwen. "Kinematics and muscle dynamics of C- and S-starts of carp(syprinus carpio L.)". Journal of Experimental Biology, 202, 1999, pages 393-406.

[8] J. Liu and H. Hu, Building a 3D Simulator for Autonomous Navigation of Robotic Fishes, Proceedings of IEEE/RSJ Int. Conf. on Intelligent Robots and Systems, Sendai International Centre, Sendai, Japan, 28 Sept. - 2 Oct. 2004, pages 613-618.

[9] J.Z. Yu, etc. A simplified Propulsive Model of Biomimetic Robot Fish and Its Realization. IEEE Transactions on Systems, Man and Cybernetics Part B: Cybernetics, Vol. 34, No. 4, 2004, pages 1798-1810.

[10] E.G. Drucker and G.V. Lauder. Wake dynamics and fluid forces of turning maneuvers in sunfish. Journal of Experimental Biology, 204, 2001, pages 431-442.